



Molecular Crystals and Liquid Crystals Science and Technology. Section A. Molecular Crystals and Liquid Crystals

Publication details, including instructions for authors and subscription information:

<http://www.tandfonline.com/loi/gmcl19>

Point Defects in Mesophases: A Comparison Between Dilatometric and Small Angle X-Ray Scattering Studies

Anne-Marie Levelut^a, Stéphane Deudé^a, Stéphan Megtert^{a,b}, Denis Petermann^a & Jacques Malthête^c

^a Laboratoire de Physique des solides, CNRS-UMR 8502, Université Paris-Sud, F-91405, Orsay, Cédex

^b LURE, CNRS-UMR 130, Université Paris-Sud, F-91898, Orsay, Cédex

^c Institut Curie, Section de Recherche, CNRS-UMR 168, 11, rue P.-et-M. -Curie, F-75231, Paris, Cédex

Version of record first published: 24 Sep 2006

To cite this article: Anne-Marie Levelut, Stéphane Deudé, Stéphan Megtert, Denis Petermann & Jacques Malthête (2001): Point Defects in Mesophases: A Comparison Between Dilatometric and Small Angle X-Ray Scattering Studies, Molecular Crystals and Liquid Crystals Science and Technology. Section A. Molecular Crystals and Liquid Crystals, 362:1, 5-21

To link to this article: <http://dx.doi.org/10.1080/10587250108025757>

PLEASE SCROLL DOWN FOR ARTICLE

Full terms and conditions of use: <http://www.tandfonline.com/page/terms-and-conditions>

This article may be used for research, teaching, and private study purposes. Any substantial or systematic reproduction, redistribution, reselling, loan, sub-licensing, systematic supply, or distribution in any form to anyone is expressly forbidden.

The publisher does not give any warranty express or implied or make any representation that the contents will be complete or accurate or up to date. The accuracy of any instructions, formulae, and drug doses should be independently verified with primary sources. The publisher shall not be liable for any loss, actions, claims, proceedings, demand, or costs or damages whatsoever or howsoever caused arising directly or indirectly in connection with or arising out of the use of this material.

Point Defects in Mesophases: a Comparison Between Dilatometric and Small Angle X-Ray Scattering Studies

ANNE-MARIE LEVELUT^{a*}, STÉPHANE DEUDÉ^a,
STÉPHAN MEGTERT^{ab}, DENIS PETERMANN^a and
JACQUES MALTHÊTE^c

^aLaboratoire de Physique des solides, CNRS-UMR 8502, Université Paris-Sud, F-91405 Orsay Cédex, ^bLURE, CNRS-UMR 130, Université Paris-Sud, F-91898 Orsay Cédex and ^cInstitut Curie, Section de Recherche, CNRS-UMR 168, 11, rue P. -et-M. -Curie, F-75231 Paris Cédex 05

Small angle X-ray scattering (SAXS) studies have been performed in the columnar hexagonal and nematic mesophases of a 1,3-diacylaminobenzene. In both mesophases the molecules are self-assembled into columns by hydrogen bonds. The SAXS experiments confirm the existence of point defects in both phases. The generic π defect is the point where a single molecule is linked to three distinct half columns. In the hexagonal columnar phase single defects are progressively replaced by pairs of π defects of opposite orientations as temperature increases and the nematic phase contains only pairs of π defects. The comparison of SAXS and dilatometric experiments provides the structure factor, the volume and the concentration of each kind of defect.

Keywords: Columnar nematic transition; point defects in mesophases; Small angle X-ray scattering

I. INTRODUCTION

For smectic or columnar mesophases with some periodic order, the comparison of the periods with the molecular dimensions is a starting point in the understanding of the average structure. However, this information must be completed by the knowledge of other molecular properties. A precise measure of the molecular volume provides important information. A. Skoulios and coworkers are among the first who got a better insight of the molecular packing in mesophases by using dilatometric experiments in addition of structural investigations by

* Corresponding Author: Tel.: 33(0)1 6915 5394; Fax: 33(0)1 6915 6086; e-mail: levelut@lps.u-psud.fr

X-ray diffraction methods^[1]. For example, in a smectic A phase, it is possible to compare the layer spacing to the molecular length and then to deduce the average area of a molecular section perpendicular to the director from the knowledge of the molecular volume. This kind of analysis has been extended to a full sequence of smectic phases^[1a]. In fact the knowledge of the molecular volume is also useful for the determination of the degree of perfection of a structure especially for crystalline solids, and eventually for some mesophases.

The concept of point defect in a pure material is attached to the solid state: in a perfect molecular crystal, the content of each unit cell is the same. The number of molecules per unit cell is an integer, Z_0 . If some unit cells, dispatched randomly, have a different content, including foreign molecules or a number of molecules different from Z_0 , then we have an imperfect crystal. In the second case, the average number of molecules per unit cell, $Z = \frac{\rho V_0}{M}$ (where ρ is the density, V_0 is the unit cell volume, and M the mass of the molecule) is no more an integer, and the difference $(Z - Z_0)$ measures the concentration of added molecules. Moreover, the local modulation of the electronic density induced by point defects results in a diffuse X-ray scattered intensity $I_d(Q) \propto c(1-c)|F(Q)-F_d(Q)|^2$, where $F(Q)$ is the structure factor of a regular site, $F_d(Q)$ the structure factor of a defect site and c the defect concentration. For single interstitials or for single vacancies $|F(Q)-F_d(Q)| = F(Q)$. This contribution is independent of the scattering vector length at least for $Q \ll 2\pi/a$, a being of the order of the molecular dimensions.

Considering a molecular fluid without any periodic order (an isotropic liquid or a nematic mesophase), it is still possible to divide the sample into small cells as in the crystal. However, the number of molecules per cell fluctuates from cell to cell and changes with time in a given cell. There are no more point defects except if the system contains some impurities. The relative amplitude of the density fluctuations decreases as the size of the cell increases. Small angle X-ray scattering (SAXS) experiments are sensitive to large-scale density fluctuations. These density fluctuations are related to the isothermal compressibility of the liquid, and the corresponding scattered intensity at small scattering angle is constant: $I(Q \rightarrow 0) \propto k_B T \rho \beta_T |F(Q)|^2$, where k_B is the Boltzmann constant, T the absolute temperature, ρ the density of the liquid, β_T the isothermal compressibility and $F(Q)$ the molecular structure factor^[2]. Let us remark that, in a nematic phase, the amplitude of the SAXS signal must be comparable to that of the isotropic liquid, however the anisotropy of the phase might be reflected in the anisotropy of the signal.

By measuring the energy transfer of the scattering process, it is possible (for example, in a Brillouin spectroscopy experiment) to discriminate between two

kinds of density fluctuations. Collective acoustic longitudinal waves are responsible for an inelastic scattering process due to Doppler effect. The intensity of the signal is proportional to the isentropic compressibility β_S . There is also a quasi-elastic component (Rayleigh scattering) proportional to $(\beta_T - \beta_S)$. The Rayleigh scattering takes into account density fluctuations, which results from long distance molecular displacements (self-diffusion). In an X-ray diffraction experiment, it is impossible to discriminate between the two terms but the Rayleigh contribution is in general dominant. In the solid phase too, there is a contribution from the acoustic longitudinal waves to the signal, whereas transverse waves do not scatter X-rays in the central Brillouin zone. Point defects give rise to an elastic signal which is generally weak compared to the contribution of thermal origin. Altogether, the small angle scattered intensity increases by approximately one order of magnitude as the compound melts.

We may wonder whether "density point defects" can exist in thermotropic liquid crystalline phases. Here, by point defects we mean regions of small volume (i.e. less than ten times the molecular volume), the density of which is higher or smaller than the average density. Intuitively we can assume that if translational diffusion is important, then a small region of a different molecular density will have a small life time and will be nothing more than a density fluctuation in equilibrium with the environment. Consequently, point defects can be found in a rather stiff phase such as an ordered smectic phase or a columnar phase. The columnar phase is an assembly of parallel stacks of molecules, generally of a disc shape, which are located at the nodes of a 2D lattice. In the perfect material, the columns extend over the whole sample. However, it may happen that some of these columns end inside the sample, introducing then a defect region at their end; J. Prost described such column ends^[3].

A column end induces a local distortion of the lattice, and if a large number of defects are introduced in the phase, the correlation length of the periodic order becomes comparable to the average distance between defects. On heating, the columnar phase then transforms into a nematic phase in which some columnar organization might persist on a local scale. In fact, the nematic phase of disc-like molecules usually does not have long columnar clusters. Such column clusters must be stabilized either by an intermolecular hydrogen bond network^[4], or by the strong interaction between electron donors and acceptors in charge transfer complexes^[5].

Long columnar clusters have been seen in the nematic phase of 1,3-diacylamino benzenes^[4] (Fig. 1). The formation of the columns is due to hydrogen bonds which link together the amide groups of neighboring molecules. The average distance between molecules in a column and the average column diameter can both be measured by X-ray diffraction. From these dimensions, it appears that the col-

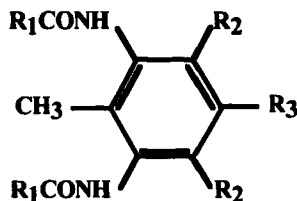


FIGURE 1 General chemical formula of 1,3-diacylaminobenzenes^[4]; R_1 = alkyl chain; R_2 = $-\text{CH}_3$; R_3 = $-\text{H}$. R_1 = alkyl chain; R_2 = $-\text{H}$; R_3 = *tert*-butyl. R_1 = alkyl chain; R_2 = $-\text{H}$; R_3 = $-\text{CO}_2$ -alkyl or alkenyl chain. Compound 1: R_1 = $-\text{C}_{15}\text{H}_{31}(\text{n})$; R_2 = $-\text{H}$; R_3 = $-\text{CO}_2\text{C}_8\text{H}_{17}(\text{n})$

umn section corresponds to an average number of molecules between 1 and 2, depending on the compound studied. Another important feature of the nematic phase of 1–3 diacylamino benzenes is its unusually large value of the orientational order parameter ($S \approx 0.9$). The structure is similar to that of main chain nematic polymers. Moreover, the properties of the nematic columnar phase can be compared to those of the lyotropic nematic phases of rigid polymers such as PBLG, DNA, etc....

A transition between a hexagonal columnar and a nematic phase, is observed on *n*-octyl *N,N'*-bis-(3,5dipalmitoylamino)4-methylbenzoate (1) and the nematic phase is, beyond any doubt, a columnar nematic one^[6]. The transition temperatures (in °C) of this compound as determined by DSC on a heating cycle are:



Moreover, in this case we were able to prove the existence of localized defects. The hexagonal lattice of the columnar phase is preserved at a local scale in the nematic phase and the average distances between molecules are well defined in every direction and in the whole mesophase temperature range. Therefore, it is possible to define a unit cell volume V_x and to compare it to the molecular volume V_m measured by dilatometry^[6]. The nature of the defects (interstitials or vacancies) and their concentration is derived from the ratio $(V_x - V_m)/V_x$. In the nematic phase, 15% of the molecules are on interstitial sites. In the hexagonal phase $(V_x - V_m)$ is close to zero and a sign inversion occurs: we have measured a maximum of 0.5% vacancy sites in the metastable supercooled hexagonal phase.

In fact the comparison of V_x and V_m provides information about the total volume of defect sites, but the volume and the structure of each kind of defect are not known. In order to obtain a better image of the defects and of their role in the phase transition mechanism we decided to performed SAXS experiments, that is for $|Q| \leq \pi/a$ where a is the hexagonal lattice constant. After a description of the

experimental set-up, we will show the experimental results. Then we will reconsider the structure of the defects in the light of the SAXS experiments.

II. EXPERIMENTAL SET-UP

A SAXS experimental set-up specially designed for liquid crystals must meet specific criteria.

- First of all, we may expect an anisotropic signal. Thus we need a beam of circular section associated to an area detector.
- The second important point is the fact that the Q range must be one order of magnitude lower than that probed in similar experiments on simple fluids such as water. In columnar mesophases, the column diameter is of the order of 20–40 Å. Therefore, if we want to explore the first Brillouin zone, the upper limit in Q is about 0.1–0.2 Å⁻¹. With a lower limit of the order of 0.01 Å⁻¹, we will be able to measure density fluctuations extending over about 20 molecules or less.
- In this Q range, the scattered intensity has in general a low level and we need a high signal-to-noise ratio. Moreover, the signal is supposed to be independent of the Q values, therefore we do not need a good resolution in Q , but in order to analyze our data we need to perform absolute scale measurements of the scattered intensity.

In order to produce a beam of high intensity with a small cross-section, we have used a mirror optics coupled to a Rigaku fine focus (0.1 mm × 0.1 mm) rotating (copper) anode. The beam is reflected successively by two Ni-coated crossed mirrors. Each mirror is slightly bent and the adjustable curvature compensates the natural beam divergence in two perpendicular planes. With this optics, we obtain a remarkably intense and almost parallel beam. The major drawback is the low energy resolution of the mirrors. The mirrors act as a filter that eliminates the high energy radiations. The nickel coating was designed to eliminate the K_β radiation, and we have reinforced the filtering effect by introducing a 20 μm nickel foil in the beam path. The resulting spectrum is made of the superposition of the K_α line and of a low intensity continuous spectrum sitting on the low energy side of the K_α line. A rough image can be given by the profile of a Bragg spot recorded on an image plate: the contribution of the continuous component to the total energy carried out by the beam is less than 1%.

The detector is a proportional gas (Argon-Methane) detector of large area (10 cm × 10 cm) which has been already described elsewhere^[7]. The main difference with a classical multiwire detector is that the signal is distributed between

four collectors on a cathode constituted by a resistive square plate, instead of being measured at each end of each wire. However, an array of parallel wires is placed in front of the cathode, which ensures a good charge collection over the whole cathode area. The sensitivity of the detector is modulated at the period of the wire array and the resulting raw image is very similar to that obtained with a multiwire detector.

The sample is held in a glass capillary (diameter 1 mm) introduced in an oven. The temperature is maintained within ± 0.1 K. Besides, there is also a temperature gradient of a few tenths of K resulting from the absence of thermal screens along the X-ray beam path. The oven is introduced in the gap (3 mm) of a permanent magnet, which provides an alignment field of 1 Tesla.

The sample environment, including a front slit, is put in an evacuated chamber. This chamber, which contains the beam stop, is closed at each end by thin Mylar windows; the length of the chamber can be adjusted so that the sample to detector distance varies between 300 and 1000 mm. As we want to measure very low levels of scattered intensity we must consider the scattering background produced by the glass walls of the capillary tube. We use amorphous silica tubes with a wall thickness of 0.02 mm. Silica walls have a smaller transmission coefficient than Lindemann glass walls but the scattering background is of lower intensity. A schematic view of the whole set-up is shown on figure 2.

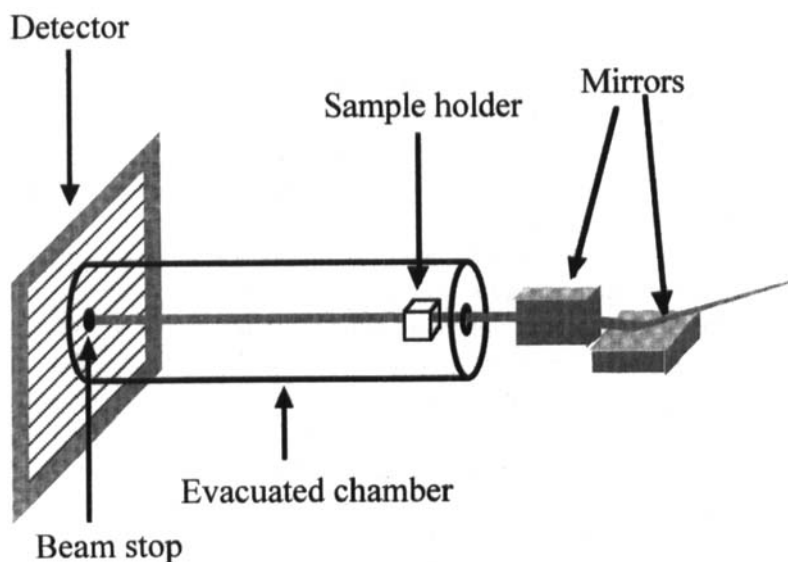


FIGURE 2 Experimental set-up

The absolute calibration of the scattered intensity is obtained from the comparison of two identical tubes, one filled with compound **1** and the second filled with water. Moreover, we have also measured the SAXS signal for a thin (0.1 mm) amorphous silica sample for a double checking test^[8]. Because we have used cylindrical cells instead of flat ones, our confidence in the absolute scattering cross-section is within $\pm 10\%$. Finally, we have also performed the same kind of experiments on the ID2 beamline at ESRF^[9], that is with a monochromatic beam. We had the same sample environment, and we used the same procedure (comparison with water) for absolute scaling.

III. EXPERIMENTAL DATA

Even though samples of compound **1** are perfectly aligned by the magnetic field, we could not detect any anisotropy of the SAXS intensity. Moreover, the signal is independent of the scattering angle in the Q range covered by our experiments. The scattering cross-section is measured on heating the sample and at each temperature the signal does not change with time (at least within a couple of hours). The data obtained with the two experimental set-ups are very similar. However, there is a systematic discrepancy of about 6% between the scattering cross-sections measured at the same temperature with the two set-ups. This difference is due to the fact that we have put the sample in a cylindrical container and not in a cell with parallel walls. In the synchrotron experiments the beam width is small compared to the container diameter whereas this is not the case with our laboratory set-up. In order to take into account this difference in beam geometry, we have systematically multiplied by 0.95 the scattering cross-sections measured with the laboratory set-up, so that the average values of both experiments can be compared.

The SAXS intensity in the hexagonal phase increases by about 20% within 10 K, on increasing temperature. The scattered intensity at small angle reaches its maximum value in the nematic phase and decreases slightly in the isotropic liquid. In fact the SAXS signal increases in the same range of temperature as the ratio $(V_x - V_m)/V_x$ which measures a defect concentration^[6]. Our small angle scattering experiments seem to confirm our previous analysis based upon dilatometric experiments (Figure 3).

Let us first comment on the notion of point defects in a mesophase. In fact the distinction between “static” defects and “dynamical” density fluctuations is not obvious. The difference is more in the specificity of the defect site than in the mobility. Here the ability of the molecules to be linked by hydrogen bonds gives the structure a polymeric character. In previous studies we took into account the

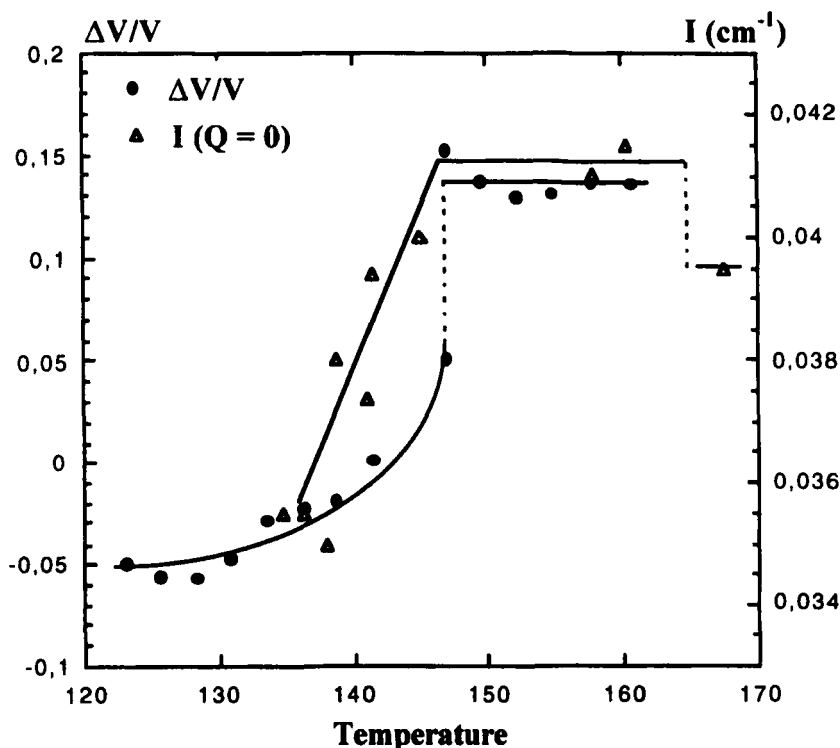


FIGURE 3 Temperature dependence of $(\Delta V/V)$, the volume fraction of defects and of I , the SAXS cross section (lines are only guides for eyes)

existence of hydrogen bonds in the description of point defects. The defect is a three branches star node, specific of the columnar organization^[6]. Three branches star nodes still exist in the isotropic phase, but the directions of the three branches are random and these defects coexist with other kinds of defects such as physical entanglements or free polymer ends. Altogether the different kinds of defects give a contribution to density fluctuations, but the great variety of the defects does not allow one to make a distinction among them.

In the mesophases, the organization in parallel columns adds the constraint that the three branches of the star must be parallel, at least at some distance from the node. They are equivalent to column ends in simple columnar phases. Moreover, they are not so labile because they are embedded in the columnar array. We can therefore consider that the defects correspond to a density modulation confined in a volume of specific shape. These defects which we call hereafter π defects because of the topology of the director field around the defective point, contrib-

ute to the small angle scattered intensity in compound **1**, in addition to the thermal fluctuations. A priori, the two kinds of contributions have a uniaxial symmetry, but since the SAXS signal is isotropic in the two mesophases, we shall assume that the two contributions are isotropic too. In a first step, we shall discuss the temperature dependence of the thermal contribution to the diffuse scattered intensity (TDS); then we shall describe the point defects specific to the mesophases of compound **1**.

IV. THERMAL DIFFUSE SCATTERING CROSS SECTION

As we have discussed previously we assume that the defects are associated to the columnar organization of the mesophase. In the isotropic phase, the distinction between the density fluctuations of dynamic origin and some static defects disappears. The system behaves like a polymer, free of impurities. Equation (1) relates the small angle scattering cross-section per unit volume $i(Q \rightarrow 0)$ in the isotropic phase to the isothermal compressibility β_t :

$$i(Q \rightarrow 0) = \sigma_e k_B T \beta_t \left(\frac{F}{V_m} \right)^2 \quad (1)$$

Where σ_e is the scattering cross-section of a free electron, F the molecular structure factor and V_m the molecular volume.

At 167.5°C, in the isotropic liquid phase, $i(Q \rightarrow 0) = 0.0395 \text{ cm}^{-1}$ and $V_m = 1468 \text{ Å}^3$, which gives $\beta_t(167.5^\circ\text{C}) = 9.95 \cdot 10^{-11} \text{ dyne}^{-1}\text{cm}^2$, which is about twice less than the isothermal compressibility of the long alkane chains in the same temperature range^[10]. The relative stiffness of compound **1** is likely due to the fact that hydrogen bonds limit the self-diffusion.

The estimation of the thermal diffuse scattering in mesophases is not obvious. The transition from the isotropic phase to the nematic phase does not disturb the local organization and especially the hydrogen bonds network. However, the total scattering cross-section per unit volume is higher in the nematic phase than in the isotropic one. This high level of scattering cross-section (about 0.0415 cm^{-1}) is probably due to the presence of defects. Let us note that after fast cooling of the sample from 167.5 to 154.5°C, the signal is lower (0.0375 cm^{-1}), corresponding therefore to a lower concentration of point defects.

The hexagonal phase can be considered as a paraffinic isotropic fluid upon which cylindrical cores are distributed on a periodic hexagonal array. This picture is in good agreement with the relative intensities of the diffraction peaks of the hexagonal lattice. According to this picture, the scattering cross-section by

unit volume is the sum of i_{ch} , the scattering cross-section of the paraffin fluid and of i_{lat} , the scattering cross-section of the periodic lattice.

The first term must be compared to density fluctuations in a pure alkane. The second term is due to the existence of a lattice: it is present around each Bragg reflection. J. V. Selinger and R. F. Bruinsma^[11] give an estimation of the phonon contribution to the SAXS signal. This contribution depends on two elastic constants, B the compressibility of the hexagonal lattice and K the bend elastic constant. The observation of grain boundaries or the analysis of the anisotropy of the TDS around the Bragg reflections provides an estimation of the ratio B/K ^[12]. K can be measured by other methods.

For compound **1** we were not able to analyze the thermal diffuse scattering intensity around Bragg peaks. First of all, we have not obtained single crystals of the columnar phase but only fiber-like samples with a fiber axis parallel to the column axis. Moreover, the intensity profile in the equatorial plane is not characteristic of a monophasic sample since a weak broad maximum is also observed at an angle lower than the Bragg angle for the hexagonal lattice. This broad diffuse ring seems to be produced by a very small amount of nematic phase which coexists with the hexagonal phase even at low temperature. This ring is close to the Bragg peak and therefore masks its TDS wings. There are no experimental measurements of the TDS contribution around the direct beam in columnar phases. However, we can compare with the cubic mesophase of a lyotropic mixture, for which the TDS signal was recorded from close to the center of reciprocal space to the second order of reflection on reticular planes^[13]: the lattice contribution of the longitudinal modes can be neglected except in the vicinity of the reciprocal nodes. In the first Brillouin zone (i. e. around the direct beam), the TDS is isotropic and equal to the TDS produced by an equivalent volume of water.

Let us assume that the thermal fluctuations in the hexagonal phase of compound **1** can be described by an isotropic compressibility, β_h . A crude estimation of β_h can be done by neglecting, in first approximation, the contribution of the defects at low temperature. At 135°C, the total scattering cross-section per unit volume of compound **1** (0.035 cm^{-1}) is lower than the computed scattering cross-section of pure alkanes at the same temperature. For example at 135°C, for dodecane, pentadecane and octadecane, the computed cross-sections^[10] are respectively 0.050, 0.048 and 0.041 cm^{-1} . The mesophases of compound **1** are stiffer than a pure paraffinic medium. As seen above, this unusual stiffness persists even in the isotropic liquid. The small amplitude of the density fluctuations in our system is likely a consequence of the limitation of molecular self-diffusion by hydrogen bonding. Considering that the structure of the fluid phase has no dramatic effect upon the density fluctuations, we shall assume that the isothermal compressibility decreases linearly with temperature until crystallization. If we

consider that the relative increment of β is similar to that of paraffin, then at 134.8°C: $\beta_h = 8 \cdot 10^{-11} \text{ dynes}^{-1} \text{ cm}^2$.

V. ANALYSIS OF THE INTENSITY SCATTERED BY THE DEFECTS

Let us recall that the global scattered intensity is independent of the modulus and of the direction of the scattering vector. This means that the defects have a volume of the order of the molecular volume (they are true point defects).

The total scattering cross-section is measured between 134.8°C in the hexagonal phase and 167.5°C in the isotropic liquid. We have a measure of the isothermal compressibility of the isotropic liquid phase. Assuming that the TDS scattering cross-section varies linearly between 0.0308 cm^{-1} at 134.8°C and 0.0395 cm^{-1} at 167.5°C, we can then deduce the scattering cross-section of the defects i_d .

V.1 Interstitial structure

Let us first consider the nematic phase. In our previous work^[6], we have considered that the nematic phase contains only interstitials. Then if F_i is the number of added electrons per interstitial, the scattering cross-section per unit volume is:

$i_i = i_i = \frac{1}{V_x} \sigma_e c_i F_i^2$. A second relation links the number of interstitials per unit cell c_i , the unit cell volume V_x , the molecular volume V_m , and the interstitial volume V_i : $c_i V_i = V_x - V_m$. Introducing, $f = \frac{V_x - V_m}{V_x}$, and $\alpha_i = \frac{V_i}{V_m}$ the scattering cross-section reads:

$$i_i = \frac{\sigma_e}{V_m} f \frac{F_i^2}{\alpha_i} \quad (2)$$

Since we cannot determine separately the size and the electronic density of the defect, we have considered two limits:

- i) the volume of the interstitial is limited to one unit cell ($\alpha_i \cong 1$). As the signal is weak the structure factor $F_i = 21$ is about 5% of the molecular structure factor ($F = 430$), which seems unlikely.
- ii) the interstitial corresponds to the addition of one molecule inside the interstitial volume. In fact, we consider that the chains of the added molecule do not contribute to the excess of electronic density brought by the defect. They rather increase the average chain electronic density. The core includes the

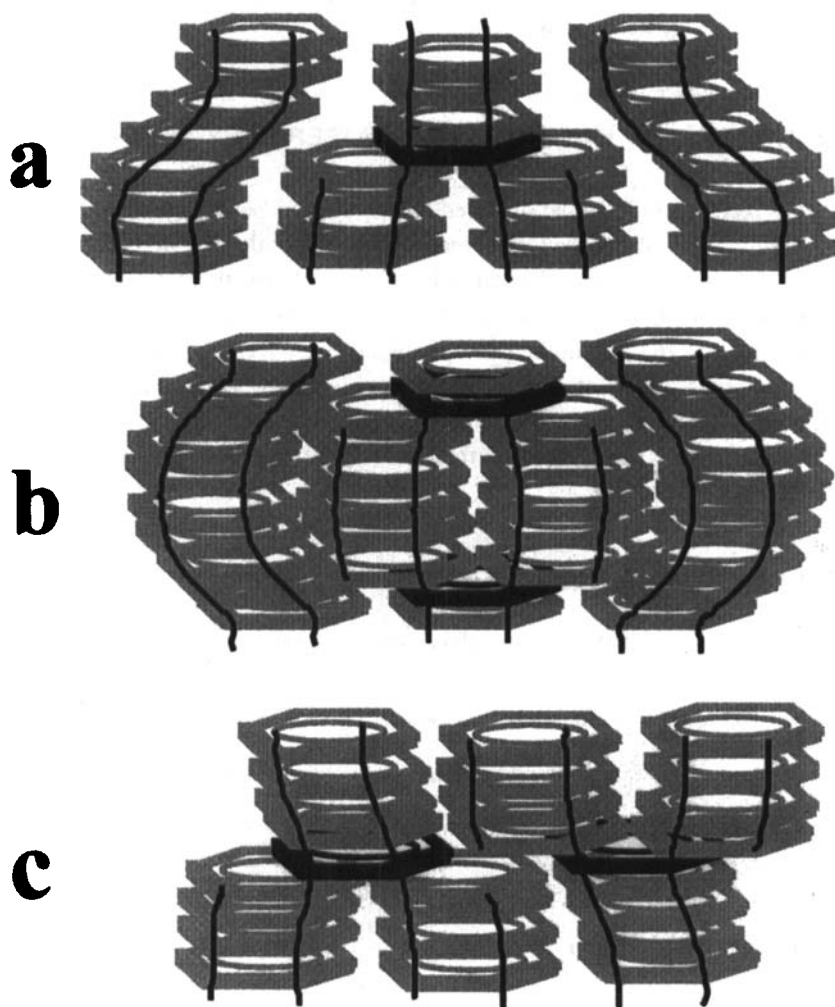


FIGURE 4 Schematic representation of a single π defect (a) and of two kinds of π defect pairs forming a loop (b) or a lock-in line (c)

phenyl ring, the carboxylic group, the two amide groups and the methyl inserted in between. Altogether, this correspond to 113 electrons which fill a circular section of radius 4 Å i.e. 50 Å^2 . The chains with 307 electrons cover an area of 320 Å^2 , and the structure factor of the interstitial is therefore $113/307(50/320) = 65$ electrons. Then α_i is equal to 7.8 and $V_i = 1.13 \cdot 10^4 \text{ Å}^3$. The interstitial volume corresponds to a sphere of about 14 Å radius. This second model seems to fit better with the molecular parameters.

The distortion surrounding the defects extends over 7 molecules along the column axis, corresponding then to a correlation length, of about 3.5 intermolecular distances. In a plane perpendicular to the column axis, the distortion around the interstitial covers approximately the area of two columns. We have considered previously that the interstitial was a lock-in line formed by the association of two elementary π defects^[6]. In fact the lock-in line^[3] is reduced to its minimum length that is two defects of opposite directions in nearest neighbor positions (fig 4c). Another possible geometry corresponds to the formation of a loop if the two defects are one above the other in a direction parallel to the column axis. The loop extends over 6–7 molecules (fig 4b). The interstitial concentration f/V_i is almost temperature independent in the nematic phase: $c_i = 1.5 \%$.

V.2 Vacancy structure

At low temperature in the hexagonal phase, there is less than one molecule per unit cell. On heating, the average number of molecules per unit cell begins to increase progressively with the temperature above 133–135°C. This number increases and becomes larger than unity close to the transition towards the nematic phase. This behavior was explained by assuming that at low temperature, the hexagonal phase contains only isolated π defects and that a single π defect is a vacancy (Fig. 4a). The number of π defects increases with temperature but simultaneously these defects form pairs, which are interstitials. Unfortunately we were not able to measure the scattering cross-section below 134°C. In fact, when the hexagonal phase is in a metastable state, we are not sure that the sample is free of crystalline seeds, during the time needed for data collection. At higher temperature, vacancies and interstitials coexist:

$$i_d = i_i + i_v = \frac{1}{V_x} \sigma_e c_i F_i^2 + \frac{1}{V_x} \sigma_e c_v F_v^2$$

$$\text{and } f - c_i V_i - c_v V_v = (\alpha_i c_i - \alpha_v c_v) V_m \quad (3)$$

The indices i and v correspond respectively to interstitial and vacancy variables. For a further analysis of our data, we assume that the formation of a vacancy corresponds to a missing core which is replaced by the paraffinic subphase: $F_v = -F_i$. We can also assume that the number of vacancies is independent of the temperature between the recrystallization temperature, 123°C, and the lowest limit of our small angle scattering experiments (about 135°C). In this temperature range, we set the value of c_v $V_v = 0.053$. This value is used to estimate i_v at 134.8 °C and 136.2 °C. Then, the average value for $\alpha_i = 3.3$ is deduced from the above equations. Moreover, between 123 and 135°C the average vacancy concentration is temperature independent and equal to 0.016 (represented by an open circle on the graph).

V.3 Temperature evolution of the defect concentration

We have all the elements for an estimation of the defects characteristics in the whole temperature range covered by the SAXS experiments. The concentrations of vacancies (i.e. single π defects), interstitials (i.e. π defect pairs) and the global concentration of π defects are reported on Fig. 5.

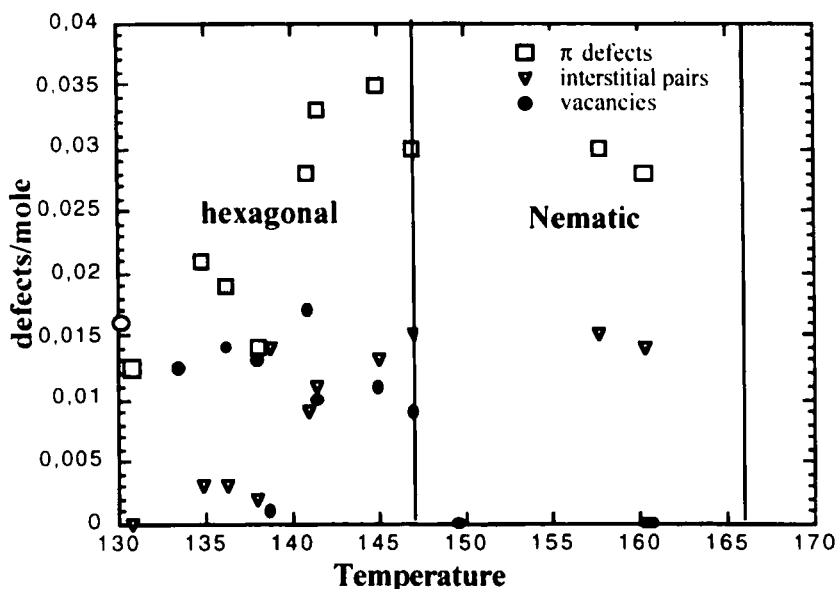


FIGURE 5 Temperature dependence of the defect concentrations

The rather large dispersion of the points, is mainly due to the poor accuracy of i_d and V_x experimental values. However, the average evolution of the three concentrations with temperature is consistent with our previous assumptions about the structure of the two kinds of defects and about their impact upon the structure of the mesophase. We have assumed that there are nearly no interstitials below 135 °C, in the hexagonal phase; above this temperature, their concentration increases progressively. More interesting is the temperature dependence of the vacancy concentration and of the total number of π defects. The hexagonal phase contains a constant number of vacancies even above 135°C. We can deduce the largest range of the attractive interactions between two π defects from the average vacancy concentration: $(0.016)^{-1/3} \approx 4$ intermolecular distances.

In the nematic phase, the defect concentration is constant. Moreover, from the volume fraction of the defects, we can deduce an average distance between

defects of about two molecular distances consistent with the previously measured correlation lengths^[6]. However, with a so short distance, interferences between defects will modify the scattering cross-section so that equation (2) may not be valid. It is possible to escape this difficulty by assuming that pairs of π defects vary in shape and in structure factor. The isotropy of the signal would result from this diversity of shape.

The estimated volume of a vacancy or of an interstitial (respectively 3.3 and 7.8 times the molecular volume) is consistent with the elastic properties of the columnar phases. Around each defect the distortion of the columns array extends over a characteristic length of the order of $\sqrt{\Lambda a}$ ^[3], where a is the hexagonal lat-

tice constant and $\Lambda = \sqrt{\frac{K}{B}}$ depends on the splay (K) and compression (B) elastic coefficients respectively. In hexagonal phases of usual disc-like molecules the characteristic length Λ is of the order of a few Å^[12]. As in solids the volume of a vacancy is less than half the volume of an interstitial. This is because an additional molecule induces a larger distorted area than a missing one. The concentration of π defects increases continuously with the temperature until the nematic phase is reached. In the hexagonal columnar phase, the vacancy concentration is constant and equal to 0.016 ± 0.002 . We can use this value for an estimation of the total number of π defects at 147°C when the two mesophases coexist: The total number of π defects is the same in the two phases. The formation of pairs favors more the nematic phase than the total number of defects. In other words, isolated defects do not disturb the hexagonal lattice as much as the lock-in lines. On the one hand, it is easy to relate the loss of the long-range hexagonal periodic order to the large distorted volume, which surrounds each lock-in line. On the other hand, the transformation of individual defects in pairs is not completely obvious. As the number of π defects increases, the distance between them decreases thus favoring the formation of pairs. However, temperature not only modifies the number of defects but also acts on the displacement of defects by a mechanism of breaking and recombination of the hydrogen bonds. Because of this complexity the system behaves like a polymer in which conformational changes are thermally activated, so that we are not sure to be in an equilibrium situation.

We have also observed that the SAXS signal depends on the thermal history of the sample, which means that the steady state is not instantaneously established. In fact, we have not performed a real study of the kinetic evolution of the system. Nevertheless, we can compare the scattering cross-sections measured during a progressive heating process to that obtained after a quick one step cooling. In the first case, the column organization is well established from the beginning of the

heating process and the number of defects increases progressively. Interestingly, intensities are the same at each temperature (within 6%) for two different experiments, which cover approximately the same range of temperature but with a difference of one order of magnitude in the average heating rate. After the series of measurements performed on the synchrotron beamline, that is with the highest heating rate, the sample was quenched within a few minutes from the isotropic phase at 167.5°C into the nematic one at 155.5°C. Then, the scattering cross-section was recorded in about 15 minutes. This scattering cross section 0.0375 cm^{-1} is higher than the estimated TDS component but the contribution of the defects is divided by a factor 2 in the quenched nematic phase compared to that measured on heating. This is the proof that the defects need time to migrate and reorganize. However, we have not simultaneously followed the position of the interference peaks and then, we have not information enough to derive a reorganization mechanism.

Moreover, it will be possible to follow the evolution of the scattering cross section at a given temperature after a temperature jump. With such experiments we might be able to obtain a better estimation of density fluctuations of thermal origin. A correct estimation is particularly important for the nematic phase where the volume fraction of defects is large. In the absence of further information on that point, we can only underline that our assumptions are justified a posteriori by the fact that the volumes and the concentrations of the two kinds of defects are consistent one with each other.

VI. CONCLUSIONS

SAXS investigations of the mesophase of compound 1 have confirmed the presence of density point defects. By putting together this new information with our previous measurements of the defect volume fraction, it is possible to have an estimation of the size of the two kinds of defects present in the sample. This system can be in a metastable state and the role of the kinetic of migration of hydrogen bonds is obvious. However, further experiments will be necessary for a more precise study of the kinetic evolution of the defects.

Acknowledgements

We would like to thank Olivier Diat for his help during the ESRF experiments.

References

- [1] a) D. Guillon and A. Skoulios, *J. phys (France)* **38**, 79 (1977);
b) M. Ibn-Elhaj D. Guillon and A. Skoulios, *Phys. Rev. A*, **46**, 7643 (1992).

- [2] A. Guinier, *X-ray Diffraction in Crystals, Imperfect Crystals and Amorphous Bodies*, Chapter 2, Dover Publication Inc., New York, USA (1994).
- [3] J. Prost, *Liq. Cryst.*, **8**, 123 (1990).
- [4] a) J. Malthête, A.-M. Levelut and L. Liébert, *Advanced Materials*, **4**, 37 (1992);
b) D. Pucci, M. Veber and J. Malthête, *Liq. Cryst.*, **21**, 153 (1996).
- [5] a) K. Praefke, D. Singer, B. Kohne, M. Ebert, A. Liebmann and J.H. Wendorff, *Liq. Cryst.*, **10**, 147 (1991);
b) H. Bengs, O. Kartaus, H. Ringsdorf, C. Baehr, M. Ebert, and J. H. Wendorff, *Liq. Cryst.*, **10**, 161 (1991).
- [6] P.-A. Albouy, D. Guillon, B. Heinrich, A.-M. Levelut and J. Malthête, *J. de Phys. II (France)*, **5**, 1617 (1995).
- [7] a) M. Lemonier, D. Petermann, D. Lefur and S. Megtert, Patent # 820344 103, France (1982);
b) C. Degert, P. Davidson. S. Megtert, D. Petermann, and M. Mauzac, *Liq. Cryst.*, **12**, 779 (1992).
- [8] A.-M Levelut and A. Guinier, *Bull. Soc. Fr. Mineral. Cristallogr.*, **40**, 445 (1967).
- [9] P. Bösecke and O. Diat, *J. Appl. Cryst.* **30**, 867 (1997).
- [10] *Handbook of Chemistry and Physics* edited by D. R. Lide, CRC press, Boston, USA 72nd edition (1991–1992).
- [11] J. V. Selinger and R. F. Bruinsma, *Phys. Rev. A*, **43**, 2910 (1991).
- [12] P. Davidson, M. Clerc, S. S. Ghosh, N. C. Maliszewsky, P. Heiney, J. Hynes Jr., A. B. Smith, *J. Phys. II (France)*, **5**, 249, (1995).
- [13] M. Imperor-Clerc and A.-M. Levelut EPJE in press (2001).